JOURNAL OF CATALYSIS **138**, 754–758 (1992)

Preparation of Precursors for the Cu/ZnO Methanol Synthesis Catalysts by Coprecipitation Methods: Effects of the Preparation Conditions upon the Structures of the Precursors

For preparation of active supported metal catalysts, the metal component is required to be highly dispersed in the precursors of the catalysts. Coprecipitation of the ingredients of the catalyst is frequently used for this purpose. Much work on the characterization of coprecipitated binary Cu/ZnO catalysts has appeared in the literature (*1–8*), since these catalysts are highly effective for the methanol synthesis and the water gas shift reaction (*9–14*).

In the present study, the precursors of Cu/ZnO catalysts with Cu/Zn molar ratios ranging from 0/100 to 100/0 were prepared from copper and zinc nitrates and $NaHCO_3$ by coprecipitation methods similar to that employed by Porta *et al.* (*5, 6*). By X-ray diffraction, differential thermal analysis, thermal gravimetric analysis, and IR spectroscopy, the structures of the precursors were found to be greatly affected by the rate of addition of the nitrates and the Cu/Zn ratio. The mechanism of the formation of the precursors was also discussed on the basis of the variation of their structures with time.

Precursors of two series of Cu/ZnO catalysts with Cu/Zn molar ratios in a range from 0/100 to 100/0 were prepared by two coprecipitation methods different in the rate of addition of a mixed solution of copper and zinc nitrates to a solution of $NaHCO_3$. Fifty cm^3 of a 1-M solution of copper and zinc nitrates was added dropwise to 100 cm^3 of a 1.2 M solution of $NaHCO_3$ (pH = 8.2) over a period of 90 min (method A) or 20 min (method B) at 338 K under continuous stirring. The precipitates formed were further aged for 90 min under stirring at the same temperature. The precipitates were then filtered out, washed, and dried at 373 K overnight. The precipitates obtained were henceforth designated as S_{An} or S_{Bn}, where A or B means the method employed, and n signifies the mole fraction of Cu multiplied by 10; i.e., 10 × Cu/(Cu + Zn). For example, S_{A3} denotes that the precipitates prepared by method A contain 0.3 mol fraction of copper.

The precursors thus prepared was analyzed by X-ray diffraction (XRD), differential thermal analysis (DTA), thermal gravimetric analysis (TGA), UV/VIS spectroscopy, and diffuse reflectance FT-IR spectroscopy. In some of runs the precipitates were collected from the solution for their characterization during the addition of a mixed solution of the nitrates or during the aging. DTA and TGA were carried out in air at a heating rate of 10 K/min. Some samples of the precipitates were decomposed in a He flow and gases evolved were analyzed by gas chromatography. Amounts of the precursors in the precipitates were determined on the basis of the integrated intensities of the XRD peaks or DTA peaks of the mechanically mixed authentic samples in variable ratios.

Figure 1a illustrates the XRD patterns of the precursors prepared by method A. S_{A10}, S_{A9}, S_{A7}, and S_{A5} show only the characteristic pattern of malachite (*15*). The peaks broaden with increased Zn content, suggesting that the crystallinity of the precursors is lowered with increased zinc content. In the reflections of S_{A3}, S_{A1}, and S_{A0}, the characteristic pattern of hydrozincite (*16*) is newly observed. With the increase of zinc

0021-9517/92 $5.00

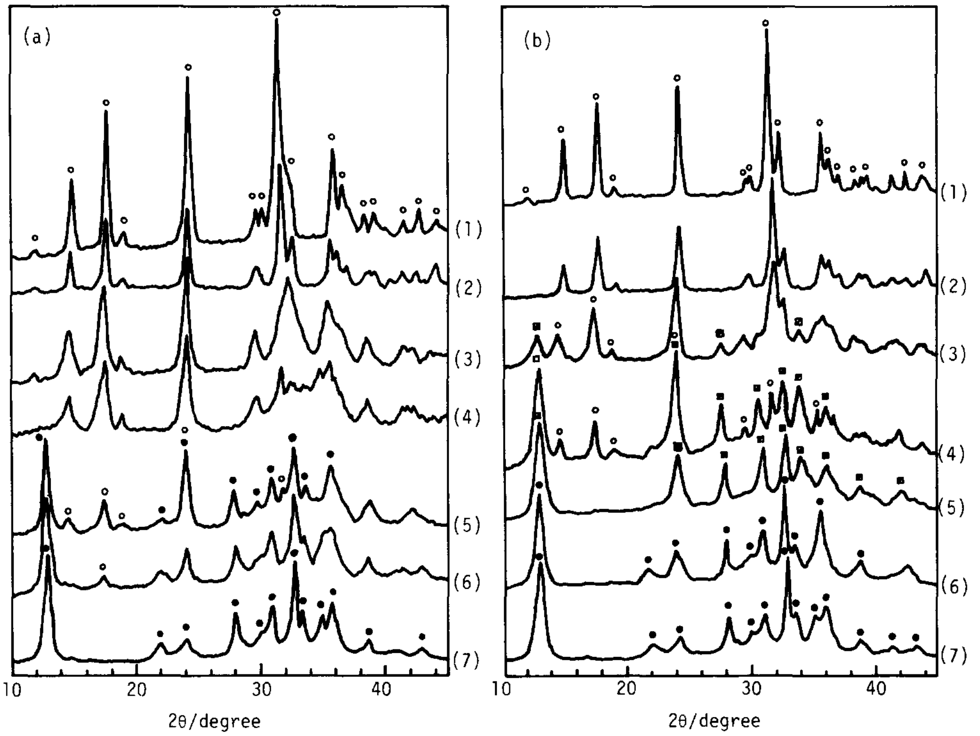

FIG. 1. XRD patterns of the precipitates prepared (a) by method A and (b) by method B. (1) Cu/Zn = 100/0, (2) 90/10, (3) 70/30, (4) 50/50, (5) 30/70, (6) 10/90, and (7) 0/100. ○, malachite; ●, hydrozincite; ▨, aurichalcite.

content the reflections of malachite decrease in intensity.

The structures of the precursors prepared by method B were different from those of the precursors prepared by method A at Cu/Zn ratios between 70/30 and 10/90. Figure 1b illustrates the XRD patterns of the precursors prepared by method B. S_{B7} and S_{B5} show the pattern of aurichalcite, $(Cu, Zn)_5(CO_3)_2(OH)_6$ (*17*), along with that of malachite. S_{B3} shows only the pattern of aurichalcite. For S_{B1} and S_{B0} only the pattern of hydrozincite is discerned.

DTA curves of the precursors are shown in Fig. 2. In accord with the XRD observations, the DTA curves vary with the Cu/Zn ratio and by the preparation method. S_{A10} and S_{B10} decompose with a sharp maximum at 576 K irrespective of the preparation method, giving CuO. This confirms that S_{A10} and S_{B10} are composed of pure malachite, $Cu_2CO_3(OH)_2$ (*5*). With the increase of zinc content to 50 mol%, this peak broadens and shifts to higher temperatures, suggesting that zincian–malachite is formed as Porta *et al.* observed (*5, 6*). S_{A0} and S_{B0} decompose with a sharp maximum at 525 K, giving ZnO. This indicates that pure hydrozincite, $Zn_5(CO_3)_2(OH)_6$, is formed. This peak shifts to higher temperature with increasing Cu content because of the formation of copper–hydrozincite (*2*). On the other hand, precursors S_{B3}, S_{B5}, and S_{B7} containing aurichalcite give a DTA peak at 600–614 K, transforming to CuO and ZnO.

The composition of the precipitates was determined on the basis of the results obtained by XRD or DTA method. Figure 3 summarizes the variation of the composition with Cu/Zn ratio for the precursors prepared by methods A and B. The composition of the precipitates with Cu/Zn ratios of

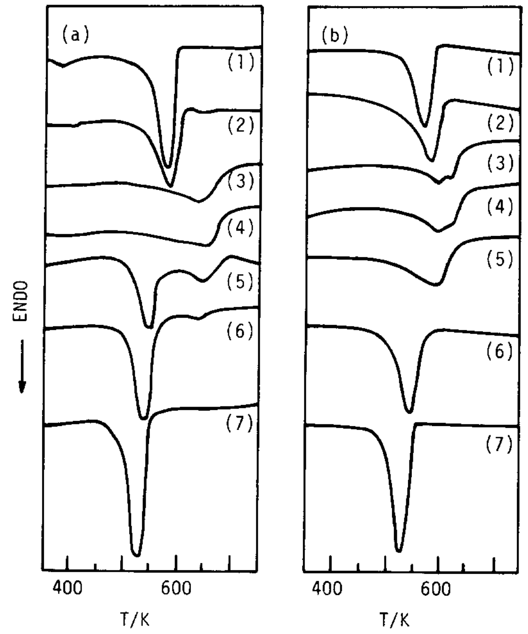

FIG. 2. DTA curves of the precipitates prepared (a) by method A and (b) by method B. (1) Cu/Zn = 100/0, (2) 90/10, (3) 70/30, (4) 50/50, (5) 30/70, (6) 10/90, and (7) 0/100.

30/70 to 70/30 depends greatly upon the preparation method, i.e., the rate of addition of the mixed solution of copper and zinc nitrates to a solution of $NaHCO_3$. The composition of the precipitates prepared by method B is in good agreement with that prepared by Porta *et al.*, although they prepared the catalysts with high Cu/Zn ratios (5).

For elucidation of the effect of the preparation method upon the structures of the precipitates, the precipitates with Cu/Zn ratio of 30/70 were sampled from the solution during the addition of the mixed solution of the nitrates and during the aging, and analyzed by XRD and DTA methods. The XRD patterns showed the presence of malachite and sodium zinc carbonate, $Na_2Zn_3(CO_3)_4$ (*18*), at the initial stage in the preparation by method A. Sodium zinc carbonate was found to convert gradually with time to hydrozincite. For the precipitates prepared by method B, sodium zinc carbonate was also detected by XRD and DTA methods. This species decreased with time and aurichalcite was formed. At the initial stage in the preparation, none of copper containing species was detected by XRD. However, the precipitates showed absorption at 800 nm ascribed to Cu(II) species in octahedral sites, strongly suggesting that the structure of copper-containing precursors was amorphous.

Similar experiments were carried out for the preparation of pure zinc or pure copper precipitates from zinc nitrate or copper nitrate. Zinc nitrate was found to convert to hydrozincite through the formation of sodium zinc carbonate irrespective of the rate of addition of zinc nitrate.

In contrast, the structure of the pure copper precipitates formed during the addition of the solution of copper nitrate was markedly affected by the preparation method.

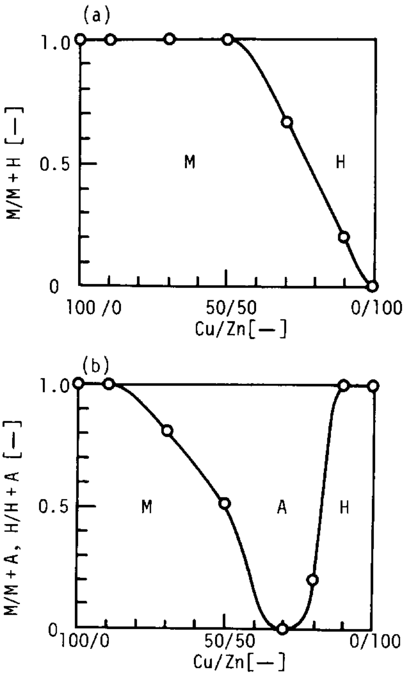

FIG. 3. Variation of the composition of precipitates with Cu/Zn ratio. Precipitates were prepared by (a) method A and (b) method B. M, H, and A represent malachite, hydrozincite, and aurichalcite, respectively.

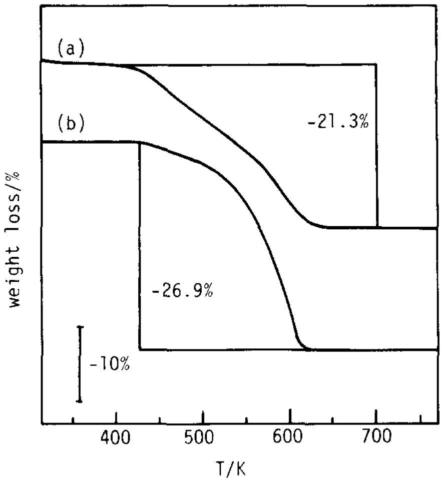

FIG. 4. TGA curves of amorphous copper precipitates. Curves (a) and (b) were obtained for the precipitates sampled respectively at 4 and 12 min in the course of the addition of a solution of copper nitrate to that of $NaHCO_3$ by method B. Percentages described in the figure represent the weight losses of the precipitates.

The precipitates formed showed the typical XRD pattern of malachite at various stages of the preparation by method A. As opposed to this, by method B, the precipitates formed at the initial stage of the preparation were amorphous in an XRD pattern. The IR spectrum of the amorphous precipitates showed strong absorptions at 1480, 1370, and 835 cm^{-1}, indicating that carbonate species were present. It was found that the precipitates decomposed to CuO, giving CO_2 and H_2O. This suggested that the amorphous precipitates were hydroxycarbonates.

Figures 4a and b show the TGA curves of the amorphous precipitates at different stages of the preparation. For the precipitates formed in the first 4 min during the course of the addition of the nitrate, the percentage of the weight loss reached 21.3% (Fig. 4a), while this reached 26.9% (Fig. 4b) for the precipitates formed in the first 12 min. On the assumption that the precipitates were hydroxycarbonate in the form $Cu_2(CO_3)_x(OH)_{4-2x}$, the composition of the amorphous precipitates was estimated from the weight losses in the TGA curves. The composition of the precipitates formed in 4 min was estimated to be $Cu_2(CO_3)_{0.27}(OH)_{3.46}$, changing to $Cu_2(CO_3)_{0.87}(OH)_{2.26}$ in the next 8 min. Upon aging, the amorphous precipitates were found to crystallize to malachite by XRD measurements. By rapid addition of the solution of copper nitrate to a solution of $NaHCO_3$, amorphous copper hydroxide, $Cu(OH)_2$, was probably formed at the initial stage of the preparation, being transformed to hydroxycarbonate species in amorphous states through the anion exchange, $2Cu(OH)_2 + xCO_3^{2-} \rightarrow Cu_2(OH)_{4-2x}(CO_3)_x + 2xOH^-$.

A mechanical mixture of the amorphous precipitates and sodium zinc carbonate was allowed to stand in a solution of $NaHCO_3$ at 338 K. The mixture was found to convert to aurichalcite. In contrast, when malachite was used instead of the amorphous precipitates, sodium zinc carbonate was merely transformed to hydrozincite. No aurichalcite was detected by XRD and DTA methods. These findings strongly suggested that aurichalcite was formed through a reaction in which the amorphous precipitates and sodium zinc carbonate were involved.

Based on these results, we concluded that in the preparation of the precursors of Cu/ZnO catalysts the difference in the rate of the addition of the mixed solution of copper and zinc nitrates to the solution of $NaHCO_3$ exerted a marked effect upon the local concentrations of the copper and the zinc cations, resulting in the difference in the initial states of the copper-containing precipitates and thereby in the final structures of the precipitates.

REFERENCES

1. Herman, R. G., Klier, K., Simmons, G. W., Finn, B. P., Bulko, J. B., and Kobylinski, T. P., *J. Catal.* **56,** 407 (1979).

2. Petrini, G., Montino, F., Bossi, A., and Garbassi, F., *in* "Studies in Surface Science and Catalysis. Preparation of Catalysts III" (G. Poncelet, P. Grange, and P. A. Jacobs, Eds.), Vol. 16, P. 735. Elsevier, The Netherlands, 1983.

3. Okamoto, Y., Fukino, K., Imanaka, T., and Teranishi, S., *J. Phys. Chem.* **87,** 3740 (1983).

4. Himelfarb, P. B., Simmons, G. W., Klier, K., and Herman, R. G., *J. Catal.* **93,** 442 (1985).
5. Porta, P., De Rossi, S., Ferraris, G., Lo Jacono, M., Minelli, G., and Moretti, G., *J. Catal.* **109,** 367 (1988).
6. Porta, P., Fierro, G., Lo Jacono, M., and Moretti, G., *Catal. Today* **2,** 675 (1988).
7. Waller, D., Stirling, D., Stone, F. S., and Spencer, M. S., *Faraday Discuss. Chem. Soc.* **87,** 107 (1989).
8. Sengupta, G., Das, D. P., Kundu, M. L., Dutta, S., Roy, S. K., Sahay, R. N., and Mishira, K. K., *Appl. Catal.* **55,** 165 (1989).
9. Kung, H. H., *Catal. Rev.-Sci. Eng.* **22,** 235 (1980).
10. Klier, K., *in* "Advances in Catalysis" (D. D. Eley, H. Pines, and P. B. Weisz, Eds.), Vol. 31, p. 243. Academic Press, New York, 1982.
11. Bart, J. C. J., and Sneeden, R. P. A., *Catal. Today* **2,** 1 (1987).
12. Ghiotti, G., and Boccuzzi, F., *Catal. Rev. Sci. Eng.* **29,** 151 (1987).
13. Chinchen, G. C., Denny, P. J., Jennings, J. R., Spencer, M. S., and Waugh, K. C., *Appl. Catal.* **36,** 1 (1988).
14. Newsome, D. S., *Catal. Rev. Sci. Eng.* **21,** 275 (1980).
15. X-ray Powder Data File, ASTM 10-399.
16. X-ray Powder Data File, ASTM 19-1458.
17. X-ray Powder Data File, ASTM 17-743.
18. X-ray Powder Data File, ASTM 1-457.

GUO CHENG SHEN
SHIN-ICHIRO FUJITA[1]
NOBUTSUNE TAKEZAWA

Department of Chemical Process Engineering
Hokkaido University
Sapporo 060 Japan

Received April 1, 1992; revised June 9, 1992

---

[1] To whom correspondence should be addressed.